



Short communication

Hierarchically porous 3D-printed akermanite scaffolds from silicones and engineered fillers

Arish Dasan^a, Hamada Elsayed^{b,c}, Jozef Kraxner^a, Dusan Galusek^d, Enrico Bernardo^{b,*}^a Dpt. Glass Processing, FunGlass, Alexander Dubček University of Trenčín, Trenčín, Slovakia^b Department of Industrial Engineering, Università degli Studi di Padova, Padova, Italy^c Ceramics Department, National Research Centre, Cairo, Egypt^d Joint Glass Centre of the IIC SAS, TnUAD, and FChFT STU, FunGlass, Alexander Dubček University of Trenčín, Trenčín, Slovakia

ARTICLE INFO

Keywords:

3D scaffolds
 Additive manufacturing
 Direct ink writing
 Polymer-derived ceramics
 Bioactive glass-ceramics

ABSTRACT

The present investigation is dedicated to the manufacturing of reticulated three-dimensional akermanite scaffolds, developed by direct reaction between silica, from the oxidation of a commercial silicone resin and oxide fillers, forming pastes for direct ink writing. Crack-free scaffolds, with dense and regular struts, were due to the use of CaCO₃ (micro) and MgO nano-particles as reactive fillers. An excellent phase purity was obtained, with the help of the liquid phase provided by anhydrous sodium borate (Na₂B₄O₇), upon firing. The structure of the scaffolds, finally, was successfully modified by using Mg(OH)₂ and hydrated sodium borate: besides macroporosity from direct ink writing, the new scaffolds exhibited homogenous 'spongy' struts (owing to water vapor release in the heating step), with no crack. Both types of scaffolds (with dense or porous struts) exhibited remarkable strength-to-density ratios.

1. Introduction

Silicate based bioceramics are particularly appreciated for their excellent bioactivity and biocompatibility [1,2]. Although several methods are available for the synthesis of silicate based biomaterials, polymer derived ceramics (PDCs) route opened a promising way to produce such bioactive materials (without compromising any biological responses), after suitable heat treatment, with a distinctive control of phase purity and microstructures [3–6].

Among silicates, akermanite (Ca₂MgSi₂O₇) ceramics have received a significant attention in the last few years due to their excellent *in vitro* bioactivity, biocompatibility and biodegradability combined with good mechanical properties [7–9]. Also in this case the synthesis may involve preceramic polymers, in the form of silicone resins filled with oxide particles: as an example, Fiocco et al. [10] reported the manufacturing of akermanite foams (82 vol% porosity and 1 ± 0.2 MPa compressive strength) by the PDCs route, which showed excellent bioactivity and biocompatibility.

A fundamental advantage of preceramic polymers is represented by the shaping possibilities. In fact, the previously mentioned polymer-derived akermanite foams were shaped at low temperature, by water vapor release in a silicone still in the polymer state; the firing did not realize only the synthesis of the desired silicate, but it also confirmed

the cellular structure achieved at low temperature [10].

In bone tissue engineering, components with a complex pore size distribution, i.e. combining macro- and micro-porosity, are favored in terms of cell attachment, growth and differentiation, and in terms of vascularization [11,12]. Well-established architectures, such as the many variants of three-dimensional reticulated scaffolds, have been revisited; the macro-porosity from the stacking of filaments have been combined with micro-porosity in the struts. A remarkable challenge concerns strut with completely open porosity, that involved a specific revision of the additive manufacturing technologies used to shape the overall scaffold structure: as an example, the direct ink writing process may be applied to emulsions instead of ceramic pastes [13–16].

The present paper discloses the potential of preceramic polymers, added with oxide fillers, in fulfilling two distinct tasks, such as the development of akermanite scaffolds, with excellent phase purity, and the obtainment of components with a hierarchical porosity. We will show that both objectives were easily achieved just by controlling the nature of fillers, in turn affecting the liquid phase formed upon firing and the gas release, determining the foaming of struts.

2. Experimental procedure

The first ink was conceived in order to achieve akermanite scaffolds

* Corresponding author.

E-mail address: enrico.bernardo@unipd.it (E. Bernardo).<https://doi.org/10.1016/j.jeurceramsoc.2019.06.021>

Received 25 February 2019; Received in revised form 5 June 2019; Accepted 9 June 2019

Available online 10 June 2019

0955-2219/© 2019 The Author(s). Published by Elsevier Ltd. This is an open access article under the CC BY-NC-ND license

<http://creativecommons.org/licenses/by-nc-nd/4.0/>.

Table 1
Detailed formulation of investigated inks (grams to obtain 10 g of final ceramic product).

Ink name	Ink composition	IPA	SiO ₂		MgO		CaO	Borax		AK glass
			FS	MK	MgO	Mg(OH) ₂		CaCO ₃	Hydrous	
Ink1	MK/FS/nMgO/mCaCO ₃	3.0	0.44	4.72	1.48	–	7.34	–	–	–
Ink2	MK/FS/nMgO/mCaCO ₃ + Akermanite glass	3.3	0.44	4.72	1.48	–	7.34	–	–	1.1
Ink3	MK/FS/nMgO/mCaCO ₃ + Na ₂ B ₄ O ₇ [dense strut]	3.1	0.44	4.72	1.48	–	7.34	–	0.16	–
Ink4	MK/FS/mMg(OH) ₂ /mCaCO ₃ + Na ₂ B ₄ O ₇ ·10H ₂ O	3.1	0.44	4.72	–	2.14	7.34	0.309	–	–

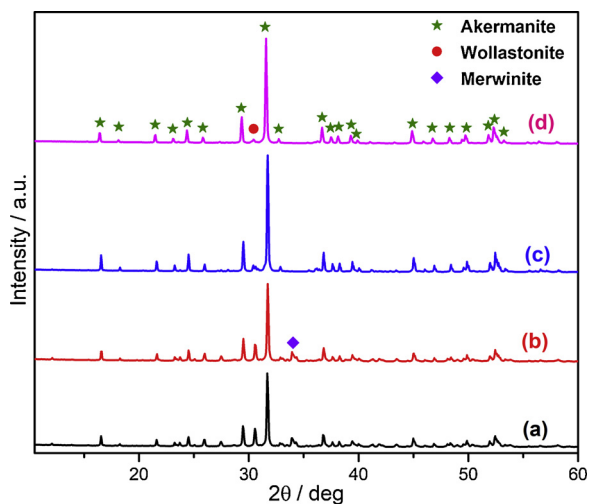


Fig. 1. XRD patterns of akermanite (AK) based 3D scaffolds a) Ak (MK/FS/nMgO/mCaCO₃); b) Ak + pure akermanite glass; c) Ak + anhydrous borax and d) Ak + borax (hydrated).

simply by reaction between polymer-derived silica and CaO- and MgO-yielding fillers. Commercially available silicone powders (MK, Wacker-Chemie GmbH, Munich, Germany) were considered as the main silica source. MK polymer was first dissolved in isopropanol (IPA) and then mixed with fumed silica (FS, Aerosil R106, Evonik, Essen, Germany), in an amount corresponding to a weight ratio between MK-derived silica and FS of 9:1. The mixing was carried out by means of a conditioning mixer (THINKY ARE-250) for 15 min at a speed of 2000 rpm/min. The specific addition of fumed silica was intended to optimize the rheology of the ink, as shown in previous direct ink writing experiments [5,6].

The MK/FS suspension in IPA was added with active oxide fillers, such as micro-sized CaCO₃ (mCaCO₃, < 10 μm, IndustrieBitossi, Vinci, Italy) and MgO (nMgO, 30 nm, Inframat Advanced Materials, Manchester, CT, USA), added in amounts corresponding to a CaO:MgO:SiO₂ molar ratio equal to 2:1:2, corresponding to stoichiometric akermanite (Ca₂MgSi₂O₇ = 2CaO·MgO·2SiO₂). The amount of silica from MK was given by its distinctive ceramic yield in air (84 wt%) [17].

A second series of inks comprised additives specifically aimed at providing some liquid phase upon firing. In analogy with recent experiences [5], the polymer/fillers mixture was modified by including

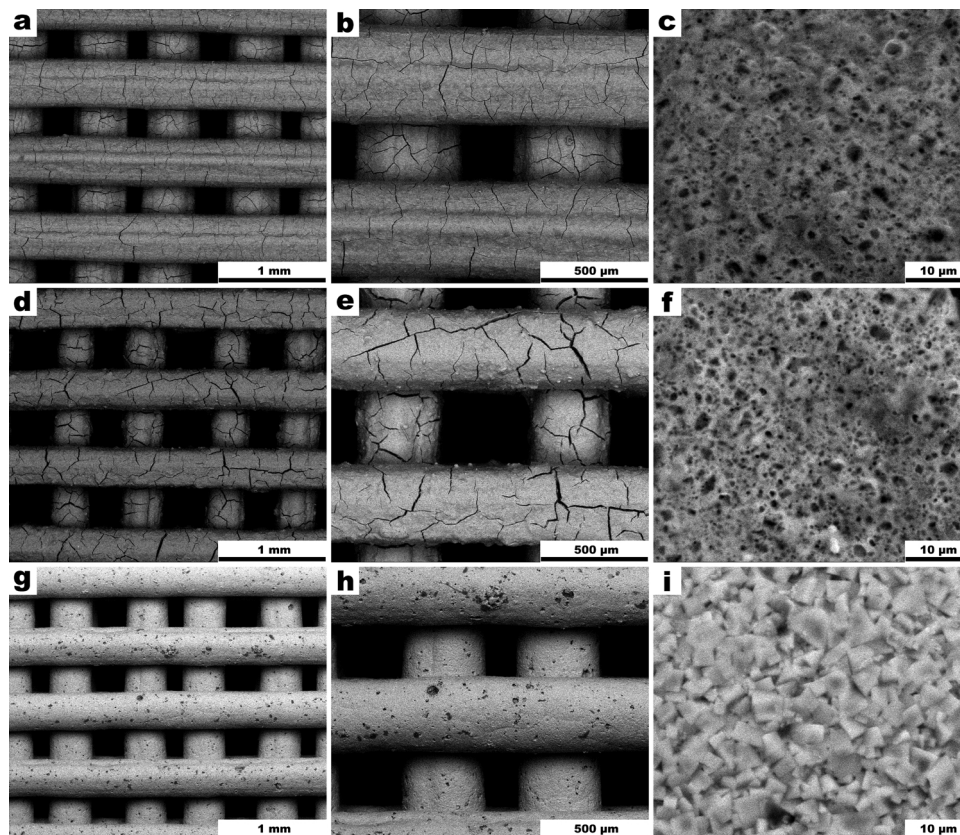


Fig. 2. Microstructural evolution (low and higher magnification images) of Ak based 3D scaffolds i) AK (a–c); ii) AK + akermanite glass (d–f); iii) AK + anhydrous borax.(g–i).

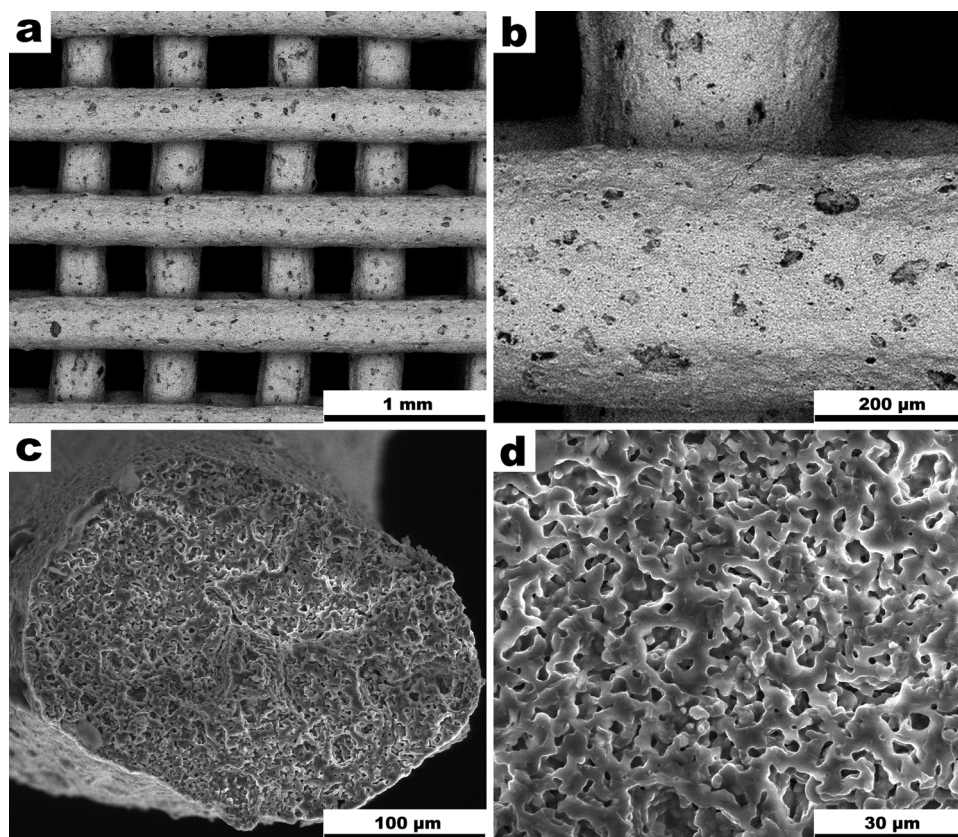


Fig. 3. SEM of images of microfoamed akermanite scaffolds printed from AK + hydrated fillers ($\text{Mg}(\text{OH})_2$ and hydrated borax): a,b) top view at low and high magnification; c,d) cross section views of spongy struts.

glass powders having the same chemical composition. An akermanite glass was produced from pure minerals and chemicals (silica, magnesium oxide, calcium carbonate - all in powders $< 10 \mu\text{m}$; all supplied by Sigma Aldrich, Gillingham, UK), by melting in a platinum crucible at a temperature of 1600°C (heating rate of $10^\circ\text{C}/\text{min}$), for 60 min.

Glass fragments, from sudden cooling of the melt on a cold metal plate, were easily reduced into fine powders by ball milling (1 h at a speed of 500 rpm/min) and manually sieved; only the particles with a diameter below $25 \mu\text{m}$ were kept. Akermanite glass powders, as an extra filler, were included in an amount of 10 wt% of the total ceramic yield of other reactants.

As an alternative, the polymer/fillers mixture was modified by including anhydrous sodium borate ($\text{Na}_2\text{B}_4\text{O}_7$, Sigma Aldrich, Gillingham, UK), for an amount of 1.5 wt% of the total ceramic yield of other reactants. For comparison purposes, this formulation was repeated by replacing nano-particles MgO with micro-particles $\text{Mg}(\text{OH})_2$, $< 10 \mu\text{m}$, Industrie Bitossi, Vinci, Italy) and anhydrous sodium borate with hydrated sodium borate (borax, $\text{Na}_2\text{B}_4\text{O}_7 \cdot 10\text{H}_2\text{O}$, Sigma Aldrich, Gillingham, UK). In order to keep the dehydration residue, corresponding to Na_2O and B_2O_3 , as 1.5 wt% of the total ceramic yield of other reactants, the reference amount of borax was raised up to 3 wt%. All details concerning the formulation of inks are reported in Table 1.

All inks were blended by means of a mixer (THINKY ARE-250), and finally loaded into a syringe and extruded through a conical nozzle ($D = 410 \mu\text{m}$, Nordson Italia S.p.a., Milano, Italy). 3D printing was performed at room temperature in air, using a commercial printer equipped with a syringe (Delta Wasp 2040 Turbo, Wasp Project, Massa Lombarda, IT). The printed scaffolds had the following geometry: $10 \times 10 \times 5 \text{ mm}^3$, with a spanning length of 1 mm between the centers of two contiguous filaments. The layer thickness was 0.35 mm to increase the adhesion between the scaffold layers. After printing, the

scaffolds were left to dry in ambient conditions. The firing treatment includes several steps as follows: preheating at 80°C for 5 h (dwelling time) in order to remove the solvents followed by 200°C for 1 h; 550°C for 3 h; 650°C for 1 h; 800°C for 3 h and finally 1100°C for 1 h. The heating rate was fixed at $0.5^\circ\text{C}/\text{min}$ in the air.

Microstructural characterizations on the ceramized scaffolds were conducted by means of optical stereomicroscopy (AxioCamERc 5s Microscope Camera, Carl Zeiss Microscopy, Thornwood, New York, USA) and scanning electron microscopy (FEI Quanta 200 ESEM, Eindhoven, Netherlands) equipped with EDS.

The apparent and true densities of the scaffolds were measured by means of a pycnometer (Micromeritics AccuPyc 1330, Norcross, GA), operating with helium gas on samples in bulk (3D printed scaffold) and powder forms. The compressive strength of sintered scaffolds was evaluated at room temperature, by means of an Instron 1121 UTM (Instron Danvers, MA) operating with a crosshead speed of $0.5 \text{ mm}/\text{min}$. The density of the ceramized scaffolds was measured geometrically using a digital calliper and by weighing with an analytical balance. Each data point represents the average value of at least 10 individual tests.

The crystalline phases were identified by means of X-ray diffraction on powdered samples (XRD; Bruker AXS D8 Advance, Karlsruhe, Germany), supported by data from PDF-2 database (ICDD-International Centre for Diffraction Data, Newtown Square, PA) and Match! program package (Crystal Impact GbR, Bonn, Germany).

3. Results and discussion

The phase assemblage of the 3D printed scaffolds is shown in Fig. 1. Akermanite ($\text{Ca}_2\text{MgSi}_2\text{O}_7$ – PDF#87-0046), as expected, was the main crystal phase in all samples. However, minor peaks corresponding to wollastonite ($\beta\text{-CaSiO}_3$ – PDF#76-0925) and merwinite ($\text{Ca}_3\text{MgSi}_2\text{O}_8$ –

Table 2
Summary of physical and mechanical properties of 3D printed glass-ceramic scaffolds.

Ink name	Scaffold formulation	Geometrical density, ρ (g/cm ³)	Open porosity, (%)	Total porosity, % [rel.density, = 1- ρ_{rel}]	Compressive strength (σ_c , (MPa) [σ_{bend}] (MPa)]
Ink1	MK/FS/nMgO/mCaCO ₃	0.81 ± 0.08	71.9 ± 2.9	72.4 ± 2.9 [ρ_{rel} = 0.276]	3.3 ± 0.6 [116]
Ink2	MK/FS/nMgO/mCaCO ₃ + Akermanite glass	0.68 ± 0.02	76.7 ± 0.7	77.1 ± 0.7 [ρ_{rel} = 0.229]	2.1 ± 0.2 [95]
Ink3	MK/FS/nMgO/mCaCO ₃ + Na ₂ B ₄ O ₇ [dense strut]	1.24 ± 0.08	56.6 ± 2.6	57.7 ± 2.6 [ρ_{rel} = 0.423]	7.3 ± 1.1 [133]
Ink4	MK/FS/mMg(OH) ₂ /mCaCO ₃ + Na ₂ B ₄ O ₇ ·10H ₂ O [spongy strut]	0.90 ± 0.03	68.7 ± 0.8	69.5 ± 0.8 [ρ_{rel} = 0.305]	4.2 ± 0.3 [124]

PDF#89-2432) emerged in the case of AK (pattern a) and pure akermanite glass added (pattern b) samples. The addition of sodium borate (pattern c), as secondary filler, had a significant impact upon ceramization, by determining the formation of nearly phase pure akermanite phase. As previously observed [3,4,10], sodium borate or sodium phosphate may promote the formation of a liquid phase upon heating, in turn, favoring the ionic interdiffusion and the crystallization of the desired phase; this extra liquid phase turns into glass phase upon cooling.

Fig. 2 shows remarkable differences also in the microstructure of the developed scaffolds. Ak (Fig. 2a,b) and Ak + glass (Fig. 2d,e) formulated scaffolds exhibited numerous cracks, due to the gas release from silicone resin and CaCO₃ upon heating. In more detail (Fig. 2c and f), the gas release was interesting in leading to ‘spongy’ struts.

The addition of pure akermanite glass as a secondary filler had been conceived firstly to enhance the liquid phase formed upon firing and secondly to heal cracks and thereby enhance the mechanical strength of the scaffolds, in analogy with earlier experiments on wollastonite-diopside glass-ceramics [6]. It is evident that the improvement in the phase purity (Fig. 1) and in the sealing of cracks were not achieved at all: akermanite glass likely crystallized just after softening, impeding faster ionic transport in liquid phase and crack healing by viscous flow.

Anhydrous borax, although determining a modification in the overall chemical formulation, on the contrary, successfully coupled phase purity with structural integrity. Despite some bubbles at the surface (Fig. 2g, h), the struts were dense and crack-free; well-packed akermanite crystals were visible at high magnification (Fig. 2i).

Borates and phosphates are actually useful for their distinctive ‘multifunctional’ character, as fillers for preceramic polymers. Besides yielding liquid phase upon firing, when used in hydrated form they may decompose into the anhydrous form, releasing water vapor at low temperature (300–350 °C), before the ceramic transformation of silicones. The release of water vapor may be enhanced considering Mg(OH)₂ instead of MgO [3,4,10].

Micro-sized Mg(OH)₂ and Na₂B₄O₇·10H₂O were effectively exploited for crack-free ‘hierarchically porous’ scaffolds, shown in Fig. 3a. The high magnification detail of Fig. 3b highlights the presence of open pores on the surface of struts, which could favor the escape of gasses from ceramic transformation. In addition, the strut cross-section was particularly uniform (Fig. 3c) and consisted of a number of interconnecting channels (Fig. 3d).

The pattern (d) in Fig. 1 shows that the introduction of the new fillers, instead of nano-sized MgO and anhydrous borax, had no negative drawback on the phase evolution: akermanite remains nearly phase pure, with just weak traces of wollastonite. It is interesting to note that the promotion of ionic interdiffusion operated by the borate liquid phase allowed for the complete incorporation of Mg²⁺ ions (there is no trace of MgO or silicate phases richer in MgO than akermanite) despite the bigger size of the Mg-yielding filler.

A summary of physical and mechanical properties of 3D printed glass-ceramic scaffolds, for different formulations, is given in Table 2. Given the differences in overall porosity, a comparison of compressive strength data may be difficult. Although more suited to truly bending dominated cellular structures (network structures with struts not overlapping with each other, but connected at nodal points), we applied the Gibson & Ashby model for strength of open-celled ceramics [18]. According to this model, the compressive strength (σ_c) is a simple function of relative density and bending strength (σ_{bend}) of the solid phase: $\sigma_c \cong 0.2 \cdot \sigma_{bend} \cdot (\rho_{rel})^{1.5}$

From the observed compressive strength values, we could infer the strength of the solid phase. This parameter was not considered as a real attribute of the material, but as a measure of ‘quality’ of the overall processing, i.e. of the integrity of struts. Samples from silicone/fillers or silicone/fillers/Ak glass were nearly identical in terms of solid (see the practical mineralogical identity in Fig. 2), but the downgrading of σ_{bend} is reasonable, given the increased number of cracks. The cracks

obviously complicated the measurement of porosity: the much lower relative density, compared to the samples from borate addition, is not simply related to the presence of pores, but likely comprises a significant contribution from the same cracks.

A more significant comparison concerns just the crack-free samples: the compressive strength values of scaffolds with dense or porous struts, although different, match well with each other in terms of the related bending strength of the solid phase (~125 MPa), which in turn is in good agreement with strength values of akermanite-based dense glass-ceramics [8,19,20]. The compressive strength values (~7 MPa and ~4 MPa for structures with dense and porous struts, respectively), in addition, compare well with those of other scaffolds for bone tissue engineering [21,22].

4. Conclusions

We may conclude that:

- Akermanite based 3D scaffolds have been successfully ‘3D printed’ by the direct ink writing of an ink composed of a preceramic polymer (MK) and reactive fillers (CaCO₃ and MgO/Mg(OH)₂);
- The structural integrity and the phase evolution could be promoted by forming liquid phase upon firing: while pure akermanite glass was unsuccessful, sodium borate, despite the limited content (1.5 wt %), led to nearly phase pure and crack-free materials;
- Borax, in hydrated form, actually played a triple role, i.e. i) it promoted the achievement of phase purity; ii) it promoted the elimination of any crack; iii) it allowed the obtainment of hierarchically porous structures, since water vapor release could occur, in 3D scaffolds, at low temperature, before the ceramic transformation;
- The formulation comprising hydrated borax may constitute the basis for the direct obtainment of a new generation of glass-ceramic scaffolds with a complex porosity distribution.

Acknowledgement

This paper is a part of the dissemination activities of the project FunGlass (Centre for Functional and Surface Functionalized Glass). This project has received funding from the European Union’s Horizon 2020 research and innovation programme under grant agreement No. 739566. Discussions with Prof. A. R. Boccaccini (University of Erlangen-Nuremberg, Germany), scientific board member (Biomaterials) of the Centre for Functional and Surface Functionalized Glass, are greatly acknowledged.

References

- [1] C. Wu, J. Chang, A review of bioactive silicate ceramics, *Biomed. Mater.* 8 (2013)

- 032001-12.
- [2] Y. Huang, C. Wu, X. Zhang, J. Chang, K. Dai, Regulation of immune response by bioactive ions released from silicate bioceramics for bone regeneration, *Acta Biomater.* 66 (2018) 81–92.
- [3] E. Bernardo, J.F. Carloti, P.M. Dias, L. Fiocco, P. Colombo, L. Treccani, U. Hess, K. Rezwan, Novel akermanite-based bioceramics from preceramic polymers and oxide fillers, *Ceram. Int.* 40 (2014) 1029–1035.
- [4] L. Fiocco, H. Elsayed, J.K.M.F. Daguano, V.O. Soares, E. Bernardo, Silicone resins mixed with active oxide fillers and Ca–Mg Silicate glass as alternative/integrative precursors for wollastonite–diopside glass-ceramic foams, *J. Non-Cryst. Sol.* 416 (2015) 44–49.
- [5] A. Zocca, G. Franchin, H. Elsayed, E. Giuffredi, E. Bernardo, P. Colombo, Direct ink writing of a preceramic polymer and fillers to produce hardystonite (Ca₂ZnSi₂O₇) bioceramic scaffolds, *J. Am. Ceram. Soc.* 99 (2016) 1960–1967.
- [6] H. Elsayed, P. Colombo, E. Bernardo, Direct ink writing of wollastonite–diopside glass-ceramic scaffolds from a silicone resin and engineered fillers, *J. Eur. Ceram. Soc.* 37 (2017) 4187–4195.
- [7] X. Ke, L. Zhang, X. Yang, J. Wang, C. Zhuang, Z. Jin, A. Liu, T. Zhao, S. Xu, C. Gao, Z. Gou, G. Yang, Low-melt bioactive glass-reinforced 3D printing akermanite porous cages with highly improved mechanical properties for lumbar spinal fusion, *J. Tissue Eng. Regen. Med.* 12 (2018) 1149–1162.
- [8] A. Najafinezhad, M. Abdellahi, S. Nasiri-Harchegani, A. Soheily, M. Khezri, H. Ghayour, On the synthesis of nanostructured akermanite scaffolds via space holder method: the effect of the spacer size on the porosity and mechanical properties, *J. Mech. Behav. Biomed. Mater.* 69 (2017) 242–248.
- [9] L. Xia, Z. Yin, L. Mao, X. Wang, J. Liu, X. Jiang, Z. Zhang, K. Lin, J. Chang, B. Fang, Akermanite bioceramics promote osteogenesis, angiogenesis and suppress osteoclastogenesis for osteoporotic bone regeneration, *Sci. Reports* 6 (2016) 22005.
- [10] L. Fiocco, S. Li, M.M. Stevens, E. Bernardo, J.R. Jones, Biocompatibility and bioactivity of porous polymer-derived Ca–Mg silicate ceramics, *Acta Biomater.* 50 (2017) 56–67.
- [11] G. Turnbull, J. Clarke, F. Picard, P. Riches, L. Jia, F. Han, B. Li, W. Shu, 3D bioactive composite scaffolds for bone tissue engineering, *Bioact. Mater.* 3 (2018) 278–314.
- [12] Y. Wen, S. Xun, M. Haoye, S. Baichuan, C. Peng, L. Xuejian, Z. Kaihong, Y. Xuan, P. Jiang, L. Shibi, 3D printed porous ceramic scaffolds for bone tissue engineering: a review, *Biomater. Sci.* 5 (2017) 1690–98.
- [13] J.A. Lewis, Direct ink writing of 3D functional materials, *Adv. Funct. Mat.* 16 (2006) 2193–2204.
- [14] C. Minas, D. Carnelli, E. Tervoort, A.R. Studart, 3D printing of emulsions and foams into hierarchical porous ceramics, *Adv. Mater.* 28 (2016) 9993–99.
- [15] M.R. Sommer, L. Alison, C. Minas, E. Tervoort, P.A. Rühls, A.R. Studart, 3D printing of concentrated emulsions into multiphase biocompatible soft materials, *Soft Matter* 13 (2017) 1794–1803.
- [16] E. García-Tuñón, G. Machado, M. Schneider, S. Barg, R.V. Belló, E. Saiz, Complex ceramic architectures by directed assembly of ‘responsive’ particles, *J. Eur. Ceram. Soc.* 37 (2017) 199–211.
- [17] H. Elsayed, A. Zocca, G. Franchin, E. Bernardo, P. Colombo, Hardystonite bioceramics from preceramic polymers, *J. Eur. Ceram. Soc.* 36 (2016) 829–835.
- [18] L.J. Gibson, M.G. Ashby, *Cellular Solids, Structure and Properties*, 2nd ed., Cambridge University Press, Cambridge, UK, 1999.
- [19] Z. Han, P. Feng, C. Gao, Y. Shen, C. Shuai, S. Peng, Microstructure, mechanical properties and in vitro bioactivity of akermanite scaffolds fabricated by laser sintering, *Biomed. Mater. Eng.* 24 (2014) 2073–2080.
- [20] P. Feng, C. Gao, C. Shuai, S. Peng, Toughening and strengthening mechanisms of porous akermanite scaffolds reinforced with nano-titania, *RSC Adv.* 5 (2015) 3498.
- [21] Y. Jung, J.J. Li, H. Zreiqat, Doped calcium silicate ceramics: a new class of candidates for synthetic bone substitutes, *Materials* 10 (2017) 153.
- [22] L.-C. Gerhardt, A.R. Boccaccini, Bioactive glass and glass-ceramic scaffolds for bone tissue engineering, *Materials* 3 (2010) 3867–3910.